

## CHAPTER 117

### WAVES ON PERMEABLE LAYERS

Toru Sawaragi<sup>1)</sup> and Ichiro Deguchi<sup>2)</sup>

#### **Abstract**

To analyze a wave attenuation on a permeable layer, we first examined the applicability of Forchheimer type equation to the fluid motion in the permeable layer through permeability tests in steady and unsteady flows. Then, we investigated the effects of a boundary shear on the surface of the permeable layer on the wave attenuation by solving boundary layer equations around the surface of the layer.

It is found that the permeability and the turbulent drag coefficient in the Forchheimer type equation in the unsteady flow are different from those in the steady flow. We showed that the Forchheimer type equation could linearize by using an equivalent linear drag coefficient formulated empirically through the permeability test. The effect of the boundary shear on the wave attenuation on the permeable layer was small compared with the effect of energy loss in the permeable layer if the thickness of the layer was relatively large.

It is also found that we can predict the wave attenuation on the permeable layer exactly when the incident wave has a strong linearity.

#### **Introduction**

When we analyze a wave deformation through a structure with permeability, we often apply a Forchheimer type equation to a fluid motion in the permeable layer. A non-linear turbulent resistance term in the equation is usually replaced by a linear resistance term based on a so-called Lorentz's law of equivalent work. Also we can linearize the equation by using a newly defined equivalent linear drag coefficient through permeability tests.

However, the wave deformations on the permeable layer that were analyzed by these methods do not always agree well with the measured wave deformation. The followings are the conceivable reasons for this disagreement:

1) Errors in the evaluation of empirical coefficients in the Forchheimer type equation in unsteady flow. Several experimental results were reported about the permeability, an additional mass coefficient and a turbulent drag coefficient of a constitution material of the permeable layer in unsteady flow. Those are obtained from the experiments under very limited conditions.

1) Professor and 2) Associate Professor, Dept. of Civil Engineering, Osaka University, Suita-city, Osaka 565, Japan

2) Disregard of the boundary shear on a surface of the permeable layer. The continuity of vertical velocity on the surface of permeable layer is satisfied in the analysis of the wave deformation of conventional potential approach. However, the continuity of horizontal velocity is not satisfied and we can not evaluate exact boundary shear.

3) Non-linear behavior of incident waves.

Objectives of this research are as follows:

- 1) To investigate the influence of unsteady property of fluid motion on coefficients in the Forchheimer type equation through unsteady and steady permeability tests. Based on the experimental results, we formulate an equivalent linear drag coefficient.
- 2) To evaluate boundary shear on the permeable layer by using a horizontal water particle velocity that is a solution of a boundary layer equation near the surface of permeable layer. We examine the influence of the boundary shear on wave attenuation.
- 3) To examine the effect of nonlinear property of incident waves on wave attenuation by carrying out a Fourier analysis of surface displacement measured on the permeable layer.

**Waves on permeable layer**

First of all, we give brief explanation of an expression of wave on the permeable layer based on the potential approach. We suppose the wave of a period  $T$  and height  $H$  propagating in the positive  $x$  direction on the permeable layer. Figure 1 illustrates a definition sketch where  $D$  is the thickness of the permeable layer,  $h$  is the depth on the permeable layer,  $(u, w)$  are the water particle velocity in  $x$  and  $z$  directions,  $\phi$  and  $p$  is the velocity potential and the pressure. We attach a subscript  $d$  to the quantity in the permeable layer.

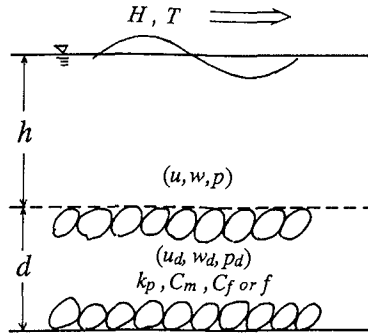


Fig.1 Definition sketch of wave on permeable layer

We can treat a fluid motion on the permeable layer as a potential flow. If we apply Forchheimer type equation to the fluid motion in the permeable layer that is expanded to the unsteady flow by Sollitt et al.(1970), we can express the fluid motion in the permeable layer as follows:

$$S \frac{\partial q}{\partial t} = -\frac{1}{\rho} \nabla p - \frac{v}{K_p} q - \frac{C_f \lambda}{\sqrt{K_p}} q^2 \tag{1}$$

$$S = \{1 + (1 - \lambda) C_m\} / \lambda$$

where  $q$  is the sectional averaged infiltration velocity (macroscopic velocity) in the permeable layer,  $\nabla p$  is the pressure gradient,  $K_p$  is the permeability of the permeable layer,  $g$  is the gravity acceleration,  $\nu$  is the kinematic viscosity of the fluid,  $C_m$  and  $C_f$  are the added mass and the turbulent drag coefficients of the rubble of the permeable layer, and  $\lambda$  is the void ratio of a permeable layer.

There are two methods to linearize the non-linear resistance term in Eq.(1). One is to determine an equivalent linear permeability by applying the Lorentz's law of equivalent work to the each layer of the horizontally divided permeable layers. We can determine a unique equivalent linear permeability  $K_{pe}$  through the whole sublayer by iterative calculations so that the total energy loss during one wave period becomes the same as that of the non-linear resistance term. However, we have to determine the values of  $C_m$ ,  $C_f$  and  $K_p$  before we find out the equivalent linear permeability and linearize Eq.(1). This method also requires large CPU time.

Another method is to use an equivalent linear drag coefficient  $f$ , which brings the same energy dispersion as that of Eq.(1) in one wave period, instead of the permeability and the turbulent drag coefficients to evaluate drag force in Eq.(1). We have to determine the value of  $f$  before we linearize Eq.(1) through the unsteady permeability test which I will mention later in detail in a next section. Anyway, in both methods, we can linearize Eq.(1) as Eq.(2) with the relation between  $K_{pe}$  and  $f$  given by Eq.(3):

$$S \frac{\partial q}{\partial t} = -\frac{1}{\rho} \nabla p - f \sigma q \quad \text{or} \quad S \frac{\partial q}{\partial t} = -\frac{1}{\rho} \nabla p - \frac{\nu}{K_{pe} \sigma} q \quad (2)$$

$$f = \gamma / (K_{pe} \sigma) \quad (3)$$

We normalize the quantities in the following manner:

$$\begin{aligned} (x', z', h', D') &= (\sigma^2/g)(x, z, h, D), \quad t' = \sigma t, \quad K_p' = \sigma K_p / \nu \\ (u', w, 'u_d', w_d') &= (1/\alpha a_0)(u, w, u_d, w_d) \\ (p', p_d') &= (1/\rho g a_0)(p, p_d), \quad (\phi', \phi_d') = (\sigma/g a_0)(\phi, \phi_d) \end{aligned} \quad (4)$$

where,  $\sigma$  is the angular frequency and  $a_0$  is the amplitude of surface displacement of a fundamental frequency component.

Then the fundamental equations to be solved are shown below.

On the permeable layer:

$$\nabla'^2 \phi' = 0 \quad (5)$$

where,  $u' = \partial \phi' / \partial x'$ ,  $w' = \partial \phi' / \partial z'$  (6)

In the impermeable layer:

$$\nabla'^2 \phi_d' = 0 \quad (7)$$

where,  $u_d' = \xi (\partial \phi_d' / \partial x')$ ,  $w_d' = \xi (\partial \phi_d' / \partial z')$  (8)

and  $\xi = K_{pe} \sigma / \nu = 1 / f$  (9)

The pressure on and in the permeable layer is expressed as follows:

$$p' = - \left[ \frac{\partial \phi'}{\partial t'} + \frac{g}{\alpha a_0} z + \frac{\sigma^2 a_0}{2g} \left\{ \left( \frac{\partial \phi'}{\partial x'} \right)^2 + \left( \frac{\partial \phi'}{\partial z'} \right)^2 \right\} \right] + \frac{C_1}{g a_0} \quad (10)$$

$$p_d' = -\phi_d' - \xi S \frac{\partial \phi_d'}{\partial t'} + C_2 \quad (11)$$

where,  $C_1$  and  $C_2$  are the constant.

The velocity potential in and on the permeable layer has to satisfy the following boundary conditions:

Kinematic boundary condition on the free surface:

$$\frac{\partial \eta'}{\partial t'} = -\frac{\sigma^2 a_0}{g} \frac{\partial \phi'}{\partial x'} \frac{\partial \eta'}{\partial x'} + \frac{\partial \phi'}{\partial z'} \quad : z' = \eta \quad (12)$$

Dynamic boundary condition on the free surface:

$$\eta = -\frac{\partial \phi'}{\partial t'} - \frac{\sigma^2 a_0}{2g} \left\{ \left( \frac{\partial \phi'}{\partial x'} \right)^2 + \left( \frac{\partial \phi'}{\partial z'} \right)^2 \right\} \quad : z' = h' \quad (13)$$

Continuity of the pressure on the surface of permeable layer:

$$p' = p_d' \quad : z' = -h' \quad (14)$$

Continuity of the vertical (macroscopic) velocity on the surface of permeable layer:

$$w' = w_d' \quad : z' = -h' \quad (15)$$

No vertical flux from the bottom:

$$w_d' = 0 \quad : z' = -(h' + d') \quad (16)$$

These equations are solved by the same way as finding the solution of Stokes waves. The author et al.(Deguchi,1988) have already derived the 2nd order solution corresponding to the Stokes 2nd order theory of the order of  $(\sigma^2 a_0/g)$ . Here we show the result of the 1st order solution for the sake of restricted space.

The dispersion relation for a sinusoidal wave with an amplitude  $a_0$ , which is expressed by Eq.(17) is given by Eq.(18).

$$\eta = \exp\{i(k' x' - t')\} \text{ or } \eta = a_0 \exp\{i(kx - \sigma t)\} \quad (17)$$

$$\sigma^2 = gk \frac{(\xi S + i) \sinh kh \cosh kd + \xi \cosh kh \sinh kd}{(\xi S + i) \cosh kh \cosh kd + \xi \sinh kh \sinh kd} \quad (18)$$

Equation (18) is correct to the 2nd order and is expressed here in a dimensional form. When the angular frequency  $\sigma$ , the water depth on permeable layer  $h$  and the thickness of permeable layer  $d$  are given, we can find the wave number on permeable layer from Eq.(18). If the wave number is a complex with a positive imaginary part, i.e.  $k = \alpha + i\beta$  and  $\beta > 0$ , the value of  $\beta$  becomes an attenuation factor of the wave on the permeable layer and we can express the surface profile of the wave as follows:

$$\eta = a_0 \exp(-\beta x) \exp\{i(\alpha x - \sigma t)\} \quad (19)$$

Figure 2 illustrates the dependency of the attenuation factor  $\beta$  on the non-dimensional permeability  $\xi$  and the value of  $d/h$ . These results are calculated by applying Lorentz's law of equivalent work to Eq.(1). The values of the coefficients in E(1) are shown in the figures.

We can see from Fig.2(a) that the attenuation factor becomes the maximum when the value of  $\xi$  is in the range of 0.2 and 0.4. This means that the optimum permeability exists to attenuate incident waves on the permeable layer. Figure 2(b) shows that the attenuation factor increases with the increase of the relative thickness of the permeable layer  $d/h$ . However, the rate of increase of the attenuation factor is small when  $d/h > 1$ . It is also found that the turbulent drag coefficient  $C_f$  also gives influence on the attenuation factor.

From these results, we can judge that the values of the coefficients in Eq.(1) (or Eq.(2)) play very important roles in the attenuation of wave on the permeable layer.

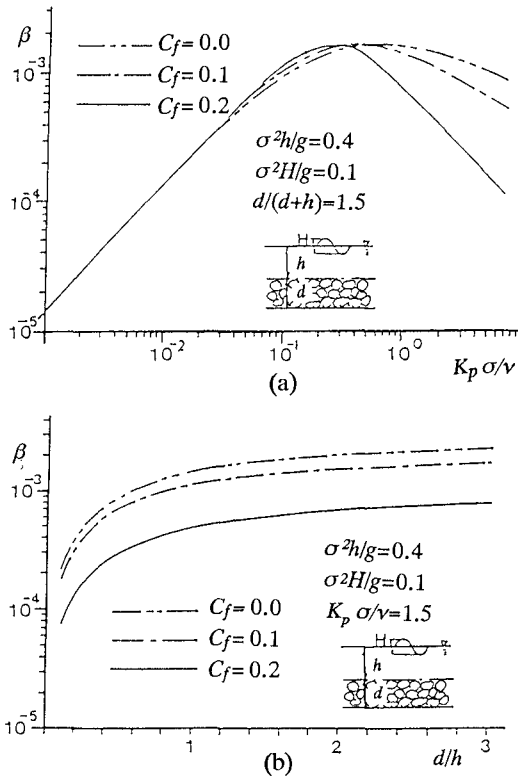


Fig.2 Dependency of attenuation factor  $\beta$  on nondimensional permeability  $\xi$  (Fig(a)) and  $d/h$  (Fig.(b)).

**Unsteady permeability test**

The author et al.(1988) have already carried out the unsteady permeability tests of rubble stones of mean grain diameter  $D=3.18cm$  and  $1.35cm$  under various flow conditions of velocity amplitude  $\hat{q}$  and period  $T$ . We found from the results that the value of  $f$  increases with the increase of K-C number ( $KC=\hat{q}/(\sigma D)$ ) and proportional to  $-1/2$  power of Reynolds' number ( $R_d=\hat{q}D/\nu$ ) when K-C number is small. It is also found that the permeability  $k_p$  in unsteady flow is almost the same as that in steady flow. However, a turbulent flow drag coefficient consists is even more small a value in unsteady flow. The added mass coefficient becomes 0 to 1.8.

However, a wave height attenuation on the permeable layer depends deeply on these coefficients. Therefore, we conducted another series of steady and unsteady permeability tests under a more extensive conditions by using rubble stones ( $D=4.50cm$ ,  $3.07cm$ , and  $1.80cm$ ). We measured a permeability  $K_p$ , added mass coefficient  $C_m$ , turbulent drag coefficient  $C_f$  and equivalent linear drag coefficient  $f$ . We also examined their dependencies on the values of  $KC$ ,  $R_d$  and so on.

The equivalent linear drag coefficient is determined from the following equation by using measured pressure gradient  $\nabla p(t)$  and sectional averaged velocity  $q(t)$  in the unsteady permeability tests:

$$f = \frac{\rho \int_t \left( -S \frac{\partial q}{\partial t} - \frac{\nabla p}{\rho} \right) q dt}{\rho \sigma \int_t q^2 dt} \quad (20)$$

An experiment was carried out by using a U-tube wave tunnel that has a straight part of 3m (0.2m wide and 0.3m high). We filled up rubbles in the middle of the straight part for 1.2m length. The amplitude of depth-averaged velocity  $\hat{q}$  and the period  $T$  of generated oscillatory flow were  $2\text{cm/s} < q < 10\text{cm/s}$  and  $5\text{s} < T < 12\text{s}$ . The corresponding ranges of  $KC$  and  $R_d$  were  $0.4 < KC < 10$  and  $360 < R_d < 4500$ .

The results are summarized as follows:

- 1) The permeability in Eq.(1) obtained from unsteady test is not always coincides with that obtained from the steady test in the region where the value of is large ( $KC > 4$ ). The former is usually larger than the latter by 20 to 50%.
- 2) The turbulent drag coefficient becomes 0 to 0.2 in the unsteady flow. This value is smaller than that in the steady flow.
- 3) The added mass coefficient becomes the maximum (1.8) when the relative acceleration defined by  $\hat{q}\sigma/g$  is about 0.01. In the region where  $\hat{q}\sigma/g$  is nearly 0 and greater than 0.04, the added mass coefficient can be regarded to be almost 0.
- 4) An equivalent linear drag coefficient does not rely on the value of  $R_d$  when the value of  $KC$  is larger than 2. The result is shown in Fig.3. It can be expressed by a unique function of  $KC$ . We can find the following empirical relation between  $f$  and  $KC$  from Fig.3.

$$f = 0.1 + 1.8 \{ \hat{q} / (\sigma D) \} \quad (21)$$

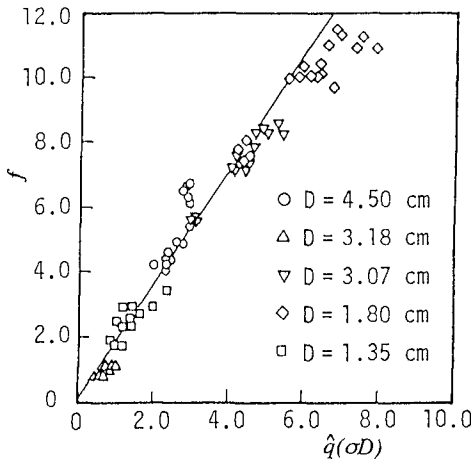


Fig.3 Relation between equivalent linear drag coefficient and K-C number

As I mentioned before, if we intend to evaluate fluid motion in the permeable layer more precisely, we should use Eq.(1) by applying the Lorentz's law of equivalent work. However, this procedure requires large CPU time until we find the

equivalent linear permeability coefficient. Also, we cannot formulate the permeability and the turbulent drag coefficient in the unsteady flow. Therefore, we use Eq.(2) together with Eq.(21) to construct boundary layer equation on and inside the permeable layer.

**Boundary shear stress on the surface of permeable layer**

(1) Boundary layer equation on and inside the permeable layer

The former analysis of the wave deformation on a permeable layer is based on a potential wave theory. Accordingly, the continuities of the pressure and vertical discharged velocity are satisfied by the imposed boundary conditions. However, the continuity of horizontal velocity is not satisfied. On the surface of the rubble on the permeable layer, a so-called non-slip condition has to be applied. A Hell-Shaw approximation is usually applied in the analysis of the steady flow on the permeable layer. However, there is no guarantee that the same approximation can apply to the unsteady fluid motion on the permeable layer.

Here, we suppose the existence of the boundary layer on and inside the permeable layer where the macroscopic horizontal velocity and the vertical gradient of horizontal velocity continue smoothly. We construct the boundary layer equations by applying Couette flow approximation in the boundary layer. Based on the analyzed results, we evaluate the boundary shear on the surface of the permeable layer and examine their effect on the wave attenuation on the permeable layer.

Figure 4 illustrates the coordinate system where,  $u_p$  and  $u_{dp}$  are the potential velocities on and in the permeable layer,  $u$  and  $u_d$  are the horizontal velocities inside the boundary layer.

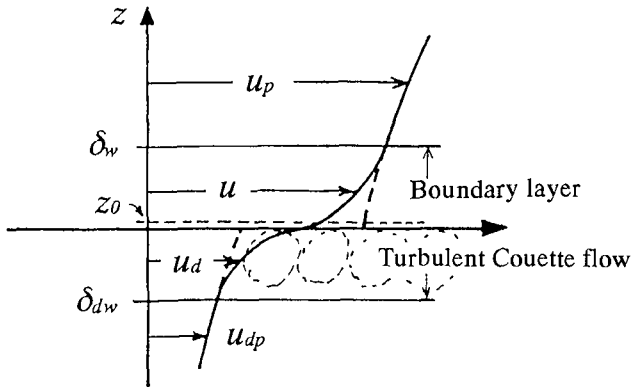


Fig.4 Coordinate system

We also assume that the thicknesses of the boundary layers on and in the permeable layer are  $\delta_w$  and  $\delta_{dw}$ , respectively and that the zero adjusting height is  $z_0$ . We need not adjust velocity distribution on the surface of the permeable layer. However, we use the expression of  $z_0$  considering the contrast of a rough turbulent boundary layer on an impermeable layer.

Then the boundary layer equations on and inside the permeable layer are expressed as follows:

The upper boundary layer,  $z_0 < z < \delta_w$ :

$$\frac{\partial U}{\partial t} = K_z \frac{\partial^2 U}{\partial z^2} \tag{22}$$

The lower boundary layer,  $-\delta_{dw} < z < z_0$ :

$$S \frac{\partial U_d}{\partial t} = -f \sigma U_d + K_{dz} \frac{\partial^2 U_d}{\partial z^2} \tag{23}$$

$$U = u - u_p, U_d = u_d - u_{dp} \tag{24}$$

where,  $K_z$  and  $K_{dz}$  are the eddy viscosity on and inside the layer.

Boundary conditions for these boundary layer equations are given by the following equations:

$$U = 0 \text{ or } u = u_p \text{ at } z = \delta_w \tag{25}$$

$$U_d = 0 \text{ or } u_d = u_{dp} \text{ at } z = \delta_{dw} \tag{26}$$

$$\partial U / \partial z = \partial U_d / \partial z \text{ or } \partial u / \partial z = \partial u_d / \partial z \text{ at } z = z_0 \tag{27}$$

$$U - U_d = u_{dp} - u_p \text{ or } u = u_d \text{ at } z = z_0 \tag{28}$$

We borrow the following expression for the kinematic eddy viscosity in Eq.(22) from the rough turbulent boundary layer theory:

$$K_z = \kappa u^* z \text{ in } z_0 < z < \delta_w \tag{29}$$

where  $u^*$  is the shear velocity on the permeable layer and  $\kappa$  is Karman's constant.

On the other hand, we express the kinematic eddy viscosity in the lower boundary layer assuming that the mixing length in the permeable layer is regulated by the scale of the void (Yamada et al.,1982):

$$K_{dz} = \gamma Du^* \text{ in } -\delta_{dw} < z \leq z_0 \tag{30}$$

where,  $\gamma$  is an empirical constant.

Through the continuity of the kinematic eddy viscosity, the order of  $\gamma$  is estimated to be as follows from Eqs.(29) and (30):

$$\gamma = \kappa z_0 / D \sim 0.4/30 \approx 0.0133 \tag{31}$$

Also, we assume that the boundary layer thicknesses of upper and lower boundary layer are expressed as follows based on the analogy of the rough turbulent boundary layer on the impermeable layer:

$$\delta_w = \delta_{dw} = \alpha \kappa u^* / \sigma \tag{32}$$

We conducted preliminary calculation as for the empirical constant  $\alpha$  and it is found that the border shearing stress becomes almost constant in the region where  $\alpha > 3$ . Therefore, we use the value  $\alpha = 4$  in the following calculation.

(2) Velocity distribution and boundary shear stress

The horizontal water particle velocities obtained as solutions to the upper and lower boundary layer equations are expressed as follows:

$z_0 < z$ :

$$u = \left[ -\beta_1 \left\{ \frac{\ker q_w + i \keiq_w}{\ber q_w + i \beiq_w} (\ber q + i \beiq) - (\ker q + i \keiq) \right\} + \beta_2 \right] \exp(-i\sigma t) \tag{33}$$

$z < z_0$ :

$$u_d = \left[ \beta_3 \exp \left\{ \frac{(a^2 + \sigma^2)^{1/4}}{b^{1/2}} \exp \left( \frac{i}{2\theta} \right) z \right\} + \beta_4 \right] \exp(-i\sigma t) \tag{34}$$

Where,

$$q_w = 2\{\delta_w \sigma / (ku \cdot)\}^{1/2}, \quad q = 2\{z \sigma / (ku \cdot)\}^{1/2}$$

$$a = f \sigma / S, \quad b = \gamma Du \cdot / S, \quad \theta = \tan^{-1}(-\sigma / a).$$

(ber, bei) and (ker, kei) are the real and the imaginary parts of the 1st and 2nd kinds of Bessel function. The integral constants  $\beta_1$ - $\beta_4$  are determined from the boundary conditions Eqs.(25) to (28).

The boundary shear stress on the surface of the permeable layer  $\tau(t)$  and the amplitude of the shear velocity  $u^*$  corresponding to the maximum shear stress  $\tau_{max}$  are evaluated by using the results.

$$\tau(t) = \rho \kappa u \cdot z_0 \frac{\partial u}{\partial z} \Big|_{z=z_0} \quad (35)$$

$$u \cdot = (\tau_{max} / \rho)^{1/2} \quad (36).$$

We can decide the water particle velocity in the boundary layers and the shear stress on the permeable layer by carrying out the same iterative calculation as in the boundary layer theory on the impermeable bed using these relations.

Figure 5 shows an example of the calculated phase variation of vertical distribution of horizontal water particle velocity in the case of J-6 that will be mentioned latter. The calculation conditions are shown in the figure.

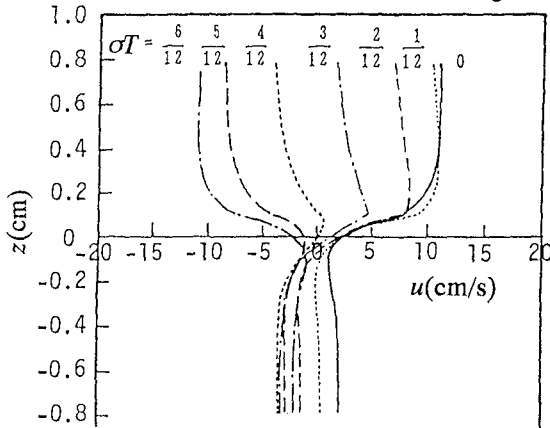


Fig.5 Example of the calculated velocity distribution

Figure 6 illustrates the effects of nonlinearity on incident waves and permeability of the layer on the boundary shear stress. The horizontal axis  $gHT^2/h^2$  of Fig.6(a) is the nondimensional parameter proposed by Shuto(1976) to show the nonlinearity of the waves of height  $H$  and period  $T$  at the depth of  $h$ . The horizontal axis of Fig.6(b) is the nondimensional permeability  $K_{pe} \sigma / \nu = 1/f$ . A calculation condition is shown in figures.

From Fig.6(a) it is found that the boundary shear stress increases in proportion to the increase of  $gHT^2/h^2$ . However, it decreases with the increase in  $1/f$  (or  $K_{pe} \sigma / \nu$ ) and becomes constant in the region of  $1/f = K_{pe} \sigma / \nu > 3$ . This region of  $1/f$  corresponds to the region where the influence of the permeability on wave attenuation decreases rapidly (see Fig.2(a)).

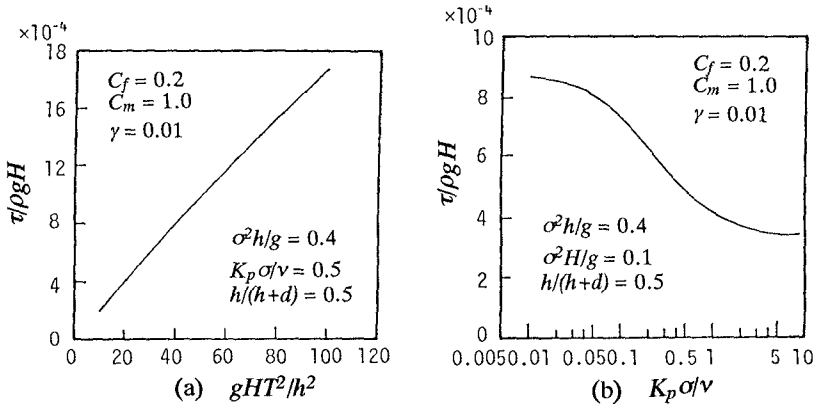


Fig.6 Effect of nonlinear property of incident wave (a) and permeability (b) on boundary shear stress

Furthermore, we examined the influence of the turbulent drag coefficient and the added mass coefficient on the boundary shear stress. As a result, the non-dimensional shear stress increases with the increases of the turbulent drag coefficient and the added mass coefficient. As for the rate of increase one of the former is big. Accordingly, that border shearing force is relying strongly on a turbulent flow drag coefficient more an addition mass coefficient was understood.

**Effect of boundary shear stress and nonlinearity of incident waves on wave attenuation on permeable layer**

(1) Experiment on wave attenuation and velocity distribution on permeable layer

We carried out experiments concerning attenuation of waves propagating on the permeable layer to investigate the effects of the boundary shear and nonlinear effect of incident waves on wave transformation on the permeable layer. The experiments were carried out on the permeable layer in the two-dimensional wave tank of 30m long, 0.7m wide and 0.9m high. The permeable layer was made on the horizontal bottom in the wave tank and the length was 3.5m and the thickness was 15cm. The water depth on the permeable layer was 15cm. Two kinds of rubble stone whose mean diameter were 3.07cm and 1.80cm were used to construct the permeable layer. Experimental conditions are summarized in Table-1.

In the experiment, We measured the water height attenuation through the permeable layer and particle velocity at the center of the permeable layer. Wave height was measured by capacitance type wave gauges at the interval of 25cm and water particle velocity was measured by an electromagnetic current meter and a hydrogen bubble method. The measured time series of surface displacement was analyzed by FFT to investigate the frequency component of wave motions. We also measured the phase difference of the water particle velocity near the boundary at the center of the permeable layer by a tuft method in 6 cases. Vertically distributed 6 pieces of silk yarn glued on the side wall of the wave tank were used as tufts.

Table-1 Experimental conditions

Case	<i>d</i> (cm)	<i>h</i> (cm)	<i>T</i> (s)	<i>H</i> (cm)	$gHT^2/h^2$
J-1	3.07	15.0	1.50	6.32	62
J-2				3.58	35
J-3			1.25	6.03	43
J-4				3.96	27
J-5			1.00	5.87	26
J-6				3.58	16
K-1		25.0	1.50	6.78	34
K-2				3.66	13
K-3			1.25	6.32	16
K-4				3.85	9
K-5			1.00	6.92	11
K-6				4.08	6
L-1	1.80	15.0	1.50	6.52	64
L-2				3.67	37
L-3			1.25	6.41	44
L-4				3.80	26
L-5			1.00	5.72	25
L-6				3.15	14
M-1		25.0	1.50	6.53	23
M-2				3.66	13
M-3			1.25	6.20	15
M-4				3.57	9
M-5			1.00	6.33	10
M-6				3.45	5

(2) Change in wave height on permeable layer

We calculated the deformation of the waves that were propagating on the permeable layer in the positive *x* direction by the following method: Let the wave heights at  $x=j\Delta x$  and  $(j+1)\Delta x$  be  $H_j$  and  $H_{j+1}$ , respectively. The wave attenuation rate  $k_p$  between  $x=j\Delta x$  and  $(j+1)\Delta x$  caused by the permeability of the permeable layer is expressed as follows:

$$k_p = \exp(-\beta\Delta x) = H_{j+1}/H_j \tag{37}$$

where,  $\beta$  is the imaginary part of the complex wave number that is the solution to the dispersion relation Eq.(18).

On the other hand, the wave attenuation rate at the same distance  $\Delta x$  caused by the boundary shear stress ( $K_t$ ) is calculated from the following equation:

$$K_t = \left[ \frac{E_t \Delta x}{H_j} \left\{ \frac{1}{16} \left( 1 + \frac{2kh}{\sinh 2kh} \right) \frac{\rho g \sigma}{k} \right\} + 1 \right]^{1/2} \tag{38}$$

where,  $E_t$  is the energy dissipation that is evaluated by using the boundary shear stress on the surface of the permeable layer as follows:

$$E_t = \frac{2}{T} \int_0^{T/2} \tau u|_{z=z} dt \quad (39)$$

Wave height at  $x=(j+1)\Delta x$  is calculated by using  $K_p$  and  $K_t$  from the wave height at  $x=j\Delta x$  by the following relation:

$$H_{j+1} = k_p k_t H_j \quad (40)$$

Figure 7 shows two examples of comparisons of measured and calculated wave attenuation in different cases. A full line is the result calculated by considering only the influence of the permeable layer by using the equivalent linear drag coefficient ( $Kt=1$ ). A broken line is the calculated result that includes both effects of the boundary shear and the permeability.

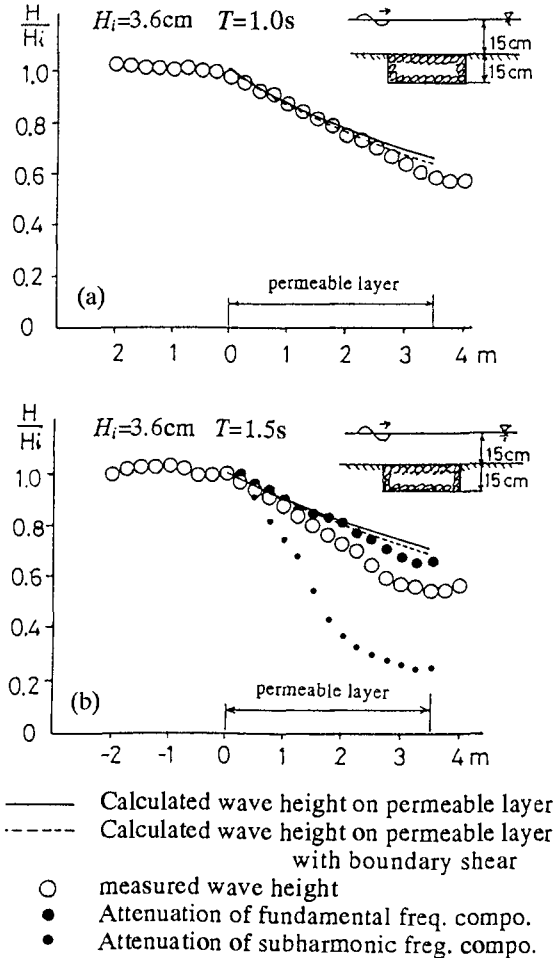


Fig. 7 Wave attenuation on a permeable layer((a):Case J-5,(b):CaseJ-2)

Figures 7(a) and (b) are the results of Case J-6( $T=1.0s$ ) and Case J-2 ( $T=1.5s$ ). Experimental conditions are shown in each figure. We used the value of the added mass coefficient in Eq.(22) obtained from the unsteady permeability tests.

First, the influence of the boundary shear on the wave attenuation, that is shown by the difference of the solid and broken lines in the both figures, is very small and can be negligible as compared with the effect of the permeability.

From Fig.7(a), it is found that measured wave height on the permeable layer (shown by the open circles) coincides fairly well with the calculated wave height when the wave period of incident waves is somewhat short. When the period is relatively long, the results of which is shown in Fig.7(b), the decrease of measured wave height on the permeable layer is larger than that of calculated one.

We investigated this reason by examining fundamental frequency and subharmonic frequency components obtained from a Fourier analysis of the measured surface displacement around the permeable layer. The energy of the subharmonic component at the offshore side of the permeable layer was less than 5% of that of the fundamental frequency component in Case J-6. On the other hand, the energy of the subharmonic component in Case J-2 was more than 30% of that of the fundamental frequency band at the offshore of the permeable layer.

In Fig.7(b), the decrease of the amplitudes of fundamental frequency and subharmonic frequency components obtained from the Fourier analysis are shown by large and small closed circles. The decrease of the amplitude of fundamental frequency component on the permeable layer agrees well with the calculated wave attenuation based on the linear wave theory. However, the decrease of the subharmonic component is larger than the predicted wave attenuation. Therefore, the difference of the measured and calculated wave heights of case shown in Figure 6 comes from the fact that a large subharmonic component was included in the incident waves.

We have already reported that the decrease of the subharmonic component in a bound wave like Storks 2nd order wave is twice as first as the decrease of the fundamental frequency component (Deguchi, et al.,1988). However, the incident waves in the case of J-2 included a larger subharmonic component that cannot be explained by the Stokes wave theory. Also, the analysis method of the wave deformation on the permeable layer based on a non-linear wave theory has been proposed (Isobe, et al.,1991). Here, we examine applicability of the linear wave theory to the wave transformation on the permeable layer.

Figure 8 illustrates errors of the calculated wave heights in the 24 cases shown in Table 1.

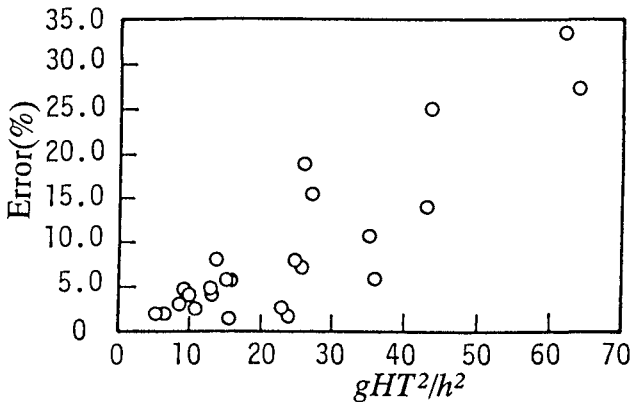


Fig. 8 Estimated error of wave attenuation on permeable layer

The horizontal axis is the parameter  $gHT^2/h^2$  concerning the nonlinearity of incident waves (Shuto, 1973). The error was defined by using the difference of measured and calculated wave attenuation rate,  $K_m$  and  $K_c$ , at the onshore end of the permeable layer as follows:

$$\delta = |K_m - K_c|/K_c * 100 \quad (26)$$

It can be seen from Fig.8 that the error becomes more than 10% when the value of  $gHT^2/h^2$  is larger than 30, i.e., the nonlinear property of incident waves is large. When the value of  $gHT^2/h^2$  is less than 10, the error remains within 5%.

## **Conclusion**

The main results obtained in this study are summarized as follows:

- 1) The turbulent drag coefficient and the permeability in the Forchheimer type equation in the unsteady flow are different from those in the steady flow. In the unsteady flow, they depend on K-C number, and the relative acceleration. We proposed the empirical relation between the equivalent linear drag coefficient and K-C number through the unsteady permeability tests.
- 2) The wave attenuation on the permeable layer is caused mainly by the energy loss in the permeable layer. The effect of the boundary shear on the surface of the permeable layer on the wave attenuation is negligibly small when the thickness of the layer is relatively large.
- 3) The linear wave theory can apply to the analysis of wave decay on the permeable layer when the value of  $gHT^2/h^2$  is smaller than 10. When the value of  $gHT^2/h^2$  is greater than 30, the non-linear property of the incident waves becomes significant. In such case, the wave attenuation on the permeable layer is larger than that predicted by the linear wave theory. We can explain this reason by the fact that the amplitude of subharmonic component included in the incident waves is faster than that of the fundamental frequency component.

## **References**

- Deguchi, I., Sawaragi, T. and Shiratani, K., 1988, "Applicability of non-linear unsteady Darcy law to wave deformation on permeable layer", Proc. 36th Japanese Conf. on Coastal Eng., pp.487-491.(in Japanese)
- Isobe, M., Shiba, K. and Watanabe, A., 1991, "Non-linear wave transformation through permeable submerged breakwater", Proc. 38th Japanese Conf. on Coastal Eng., pp.551-555.(in Japanese)
- Shuto, N., 1973, "Shoaling and deformation of non-linear long waves", Coastal Eng. in Japan, Vol.16, pp.1-12.
- Sollitt, C. K. and Cross, R.H., 1972, "Wave reflection and transmission at a permeable breakwater", Rept. Ralf Parson'S Lab., MIT, No.147.
- Yamada, M. and Kawabata, N., 1982, "Theoretical study on the resistance law for the flow on the permeable layer", Proc. JSCE, Vol.325, pp.69-80.(in Japanese)